Statistical Investigation of Dynamical Alteration In Neprilysin Related Proteins for Extracting Point of Specificity.

Journal:	*Molecular BioSystems*
Manuscript ID	MB-ART-10-2015-000727.R1
Article Type:	Paper
Date Submitted by the Author:	18-Jan-2016
Complete List of Authors:	Ul-Haq, Zaheer; ICCBS, PCMD Usmani, Saman; ICCBS, PCMD Iqbal, Sadaf; ICCBS, PCMD Zia, Syeda Rehana; ICCBS, PCMD

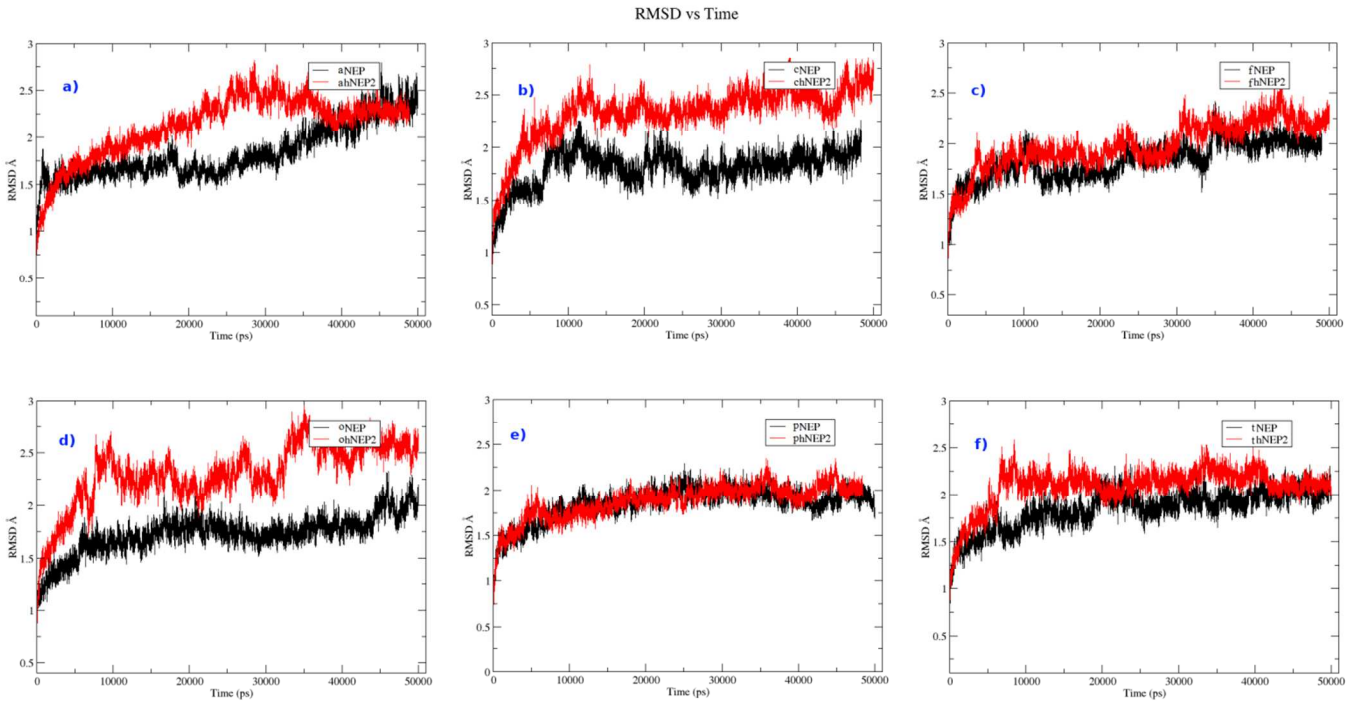

HIGHLIGHTS:

- Theoretical identification of structural changes within two related proteins during dynamics in order to obtained points for specificity. Study revealed that the compounds of hydrophilic nature can be selective inhibitors for peripheral diseases like hypertension and cardiovascular disease. However, hydrophobic can be specified for cerebral disease.

*In-Silico*Based Investigation of Dynamic Variations in Neprilysin (NEP and NEP2) Proteins for Extracting Point of Specificity

Zaheer Ul-Haq,*[a] Saman Usmani,[a] Sadaf Iqbal[b] and Syeda Rehana Zia[a]

[a]Dr. Panjwani Center for Molecular Medicine and Drug Research, International Center for Chemical and Biological Sciences, University of Karachi, Karachi-75270, Pakistan.
[b]Department of Chemistry, University of Karachi, Karachi-75270,Pakistan.

Corresponding Author:
Zaheer Ul-Haq : Email: zaheer.qasmi@iccs.edu; Tel: +92 111 222 292 Ext 309

Abstract

Neprilysin-2 (NEP2) in central nervous system controls Alzheimer's protein (amyloid-β) deposition and prevents its occurrence. However, in peripheral system, its closest homolog neutral endopeptidase (NEP) regulates hypertension and heart related diseases. Inhibitors of NEP with a lesser degree of specificity can treat hypertension with increasing risk of cerebral deposition of amyloid-β. In order to rationalize the point of selectivity, dynamic behavior of human NEP and NEP2 proteins molecular dynamics(MD) simulation was conducted. A computationally reliable model of NEP2 was achieved with 79.9%, 19.1% and 0.2% residues in allowed, additionally allowed and disallowed regions respectively, by using 1DMT as a reference protein. Additionally, molecular docking studies were careened out for a set of five already known inhibitors of NEP and modeled NEP2 to obtain a comparative behaviors of the complexes. MD results highlighted their different responses along with important residues having part in ligand-protein binding. For substrate and inhibitor binding, Arg664/661 and Zn697/694 were identified as the most conserved residues. High degree flexible transitions during MD simulations were also observed in loop areas along with active site residues. Energy calculations, hydrogen bonds and their occupancy rates helped to conclude each ligand's potency towards a particular target. In most complexes of hNEP2, ligand showed weak interactions which might be due to its larger pocket size or huge conformational variations in active site residues upon complexation.In case inhibitors of small sized like thiorphan, Arg49 and Arg664 are found to be interactive to support the ligand binding in NEP while only Arg661 is solely interactive in NEP2.

Keywords: Neprilysin (NEP), Neprilysin-2 (NEP2), Molecular Dynamic (MD) Simulations, Phosphoramidon, Thiorphan, Fasidotrilat, Omapatrilat.

1. INTRODUCTION:

Neprilysin related proteins belongs to zinc bound metallopeptidase family, catalyze the metabolic inactivation of peptide hormones and neuropeptides *via* hydrolysis. Neprilysin (NEP)[1], Neprilysin-2 (NEP2)[2], endothelin converting enzymes (ECE-1[3], ECE-2[4]), X converting enzyme (XCE)[5], Kell-erythrocyte surface antigen protein[6] and product of the phosphate-regulating gene for endopeptidase on X-chromosome (PHEX)[7] are seven well known structurally related mammalian proteins. They are responsible for the regulation of neuropeptide signaling, controlling fertility, phosphate regulation and other important physiological functions. However, they also associated with pathological conditions like cardiovascular diseases, prostate cancer, hypophosphataemia, rickets, osteomalacia, disorder associated with phosphate re-absorption andvitamin D metabolism[8,9]. These protein's isoforms are analogues of each other but have different substrate specificity, proving their distinct physiological activity within the human body[10]. Their physiological actions may vary with their localization within an organs. In brain, NEP is responsible for regulation of pain controlling neuropeptides like enkephalins and substance P while in kidneys, its function is to regulate blood pressure *via* controlling levels of atrial natriuretic peptide, bradykinin and endothelin-1. NEP is produced from adipocytes and regulated by glucose and fatty acids[11-12]. By controlling lipid metabolism, fluctuating plasma levels of NEP in human body is also associated with obesity[13] and have a role in body immune system to combat infections[14]. NEP in conjunction with angiotensin converting enzyme (ACE) also participates in blood pressure regulation through hydrolysis of its monitoring factors. Dual inhibitors of NEP and ACE were found to be more effective in treating hypertension than selective ACE inhibitors[15].

Interestingly NEP2, the closest homologue of NEP is involved in the degradation of tachykinin, enzyme of human spermatozoa that was analyzed for its function in sperm motility by different experimental methods[16]. It is known that tachykinin activity is also regulatedby neprilysins therefore, hNEP2 has its own role in the reproductive system[17]. Initially, NEP2 was referred as a soluble secreted endopeptidase (SEP) and it was first cloned in 1999 from ECE-1 knockout mice[18]. Later, it also discovered from rat brain and

mouse testis as NEP-like protein (NEPLP and Nl1)[19]. However, in human, membrane-bound metalloendopeptidase (MMEL2) gene encodes human NEP2 protein with 779 amino acids having 54% structural identity to the human NEP protein[20]. Regardless of the various similarities between both proteins, differences do exist. While the substrate specificities are very similar (particularly in rodents) their localizations suggest divergent roles in the central nervous system. Unlike NEP, NEP2 is highly expressed in the testis and brain.However, NEP2 knockout mice showed reduced sperm function[21]. Furthermore, hNEP2 showed more restricted substrate specificity compared to hNEP with less activity against several vasoactive peptides[22].Involvement of NEP2 and NEP proteins in the control of cerebral amyloid-β (Aβ) levels has been comprehensively reviewed[23,24]. Among 20 known members, neprilysin family is considered as one of the major amyloid-degrading enzymes (ADEs). In enzyme knockout and transgenic mice experiments NEP2 is found to be more efficient in metabolizing Aβthan NEP[25]. Expression levels of NEP2 in brain decreases during ageing or after such pathologies as hypoxia or ischemia. Of particular interest are the NEP inhibitors thiorphan and phosphoramidon as these inhibitors induce a dramatic increase in Aβ levels in rodent[26].Hence, selective NEP inhibitors (selectivity at the homologue level) are required in order to prevent its cerebral effects. The most potent and widely used NEP inhibitors include phosphoramidon and thiorphan that show activities at nanomolar range for both enzymes. Phosphoramidon is almost equipotent against both enzymes, while thiorphan is found to be 30 times more potent against NEP than NEP2[27]. In order to rationalize the mode of binding for known NEP inhibitors against both enzymes, we have selected three inhibitors from literature.Fasidotrilat and omapatrilat, are dual inhibitors of NEP and ACE also known as vasopeptidase inhibitors, are equipotent against NEP and NEP2[27]. Synthetic derivative of thiorphan, is the third selected inhibitor and also equipotent against NEP and NEP2,evaluated by Voisin *et al.* [28].

Aresolved crystal structure of NEP in complex with phosphoramidon allow us betterunderstanding for the catalytic properties of the enzyme[29].The active site contain a zinc ion showed HExxH conserved residues and a water molecule to complete its tetrahedral geometry[30].Complexation with inhibitors, substitutes the zinc-bound water to provide space for the accommodation of upcoming ligands. On the basis of NEP and ECE-1 crystal

structures, homology models of Kell[31-32] and XCE[33] were constructed to study their active sites. Computational modeling of ECE-2 also facilitated by the literature and helped to explore the active site for the discovery of a selective inhibitor[34]. Structural modeling of *d*NEP2 from the fly origin (*Drosophila Melanogaster*) was done using NEP structure[35]. Active site modelingof human NEP2usingsequencealignmentandthecrystalstructureofNEP was performed by Voisin and colleages who found 97%identity between their activesites[28].Here, we modeled the complete structure (residues 87-799) of human NEP2 by exploiting the crystal structure of the extracellular domain of NEP[29]. MD simulations were carried out to evaluate inhibitor binding similarities and differences between two related proteins. One of its purposes is to identify the key points that can restrict the NEP inhibitor activity to the periphery to reduce the Alzheimer's chances. This is to explore the specific changes that are responsible for their selectivity towards different physiological functions and to retrieve the reason, how structurally related proteins can produce different biological actions even upon same or different substrate binding.

2. RESULTS & DISCUSSION:

Molecular basis of ligand-protein binding, hot spot residues and the interaction consistency can be appropriately explored*via* molecular dynamic (MD) simulations. It is a bioinformatics based computational toolto calculate the time dependent conformational variations of bio-molecules, even at nanosecond levels. These conformational flexibilities are associated with protein functions, thus, the activity could be explored through molecular and atomic level studies. This studywould serve the purpose of facilitating the science with valuable knowledge regarding NEP and NEP2 structural differences to prevent cerebral disturbance upon peripheral receptor blockade. Comparative protein structure modeling compensated the crystallographic structural deficiency of NEP2 when exploring its hidden features.

2.1.Homology Modeling of Human Neprilysin (hNEP2):

Homology modeling, the most appropriate tool to construct a three dimensional structure of protein through amino acid sequences, required an experimentally resolved reference structure. Here, Jalview software was used to align hNEP2 sequence on human NEP,

presented in figure-**1**, showing high sequence similarity amongst them. Rather, the active site residues only, the disulfide bridge forming cycteines were also found to be conserved having prominent role in protein folding. However, residual conservation is high in their C-terminal regions than N-terminals, ensuring that the protein subtypes characteristics lie in this region. After getting exact sequence alignment between both proteins,multiple spatial models were allowed to generate using MOE.The constructed models were then, sequentially, analyzed for their validation by Ramachandran plot through percentage occurrence of their residues in already defined; allowed, additionally allowed and disallowed regions. Finally,a model with 79.9%, 19.1% and 0.2% residues in three respective regions was selected as most appropriate, ensuring its correct and reliable modeling (figure-**2**). A large portion containing initial eighty six residues were unable to model due to lack to this part in the reference crystal structure of NEP. **H**ELT**H** and G**E**NIAD motifs contributed through their two histidines and one glutamate, respectively, to the catalytic site of neprilysin related proteins. The glutamate in close proximity of Zn, act as nucleophile to replace Zn coordinated water molecule with an inhibitor. The apo form of NEP (apo-NEP) was constructed by truncating the inhibitor; phosphoramidon,in a form that only the zinc bound oxygen atom remainsand served as zinc bound water molecule. However, the apo-hNEP2 structure was taken developedmodules.

Subsequently, the firsthNEP2-inhibitor complex was designed using the known bio-active conformation of phosphoramidon. Manual shifting of inhibitor from the co-crystallized NEP structure to modeled human NEP2 resulted in its complex with phosphoramidon (phNEP2).Moreover, appropriate ligand-protein confirmations for remaining four known inhibitors with NEP and modeled NEP2 proteins were obtained using molecular docking tool of MOE.Docking results highlighted the hotspot residues, found to be interacting, in both proteins. The interacting residues of active site are same in the both isoforms; however, the residual numbering is different due to missing structural information of starting residues in the reference protein. NEP and NEP2 prepared proteins with respect to the reference 1DMT residual numbering is displayed in table-**1**. Arg664/661 (through bidentate interactions), Asn489/486, His658/655 and Val488/485 with a strong, permanent Zn697/694 interactionare important active site residues,see figure-**3**. These modeled apo and complex

hNEP2 structures along with their respective NEP reference structures were used for long term simulationsto explore the point of specificity.

2.2 Nano-scale Molecular Dynamic Predictions:

Long term molecular dynamic simulations are considered to be valuable for proper sampling and to provide an actual set of information. Here, simulation was run for a period of fifty nanoseconds to investigate the structural differences of hNEP and hNEP2 proteins with or without ligands*via* enhanced sampling. Total two apo and ten binary complexes were allowed to simulate for 50ns.However,these MD runs were stopped at their 50^{th} nanoseconds with structural stability for at least 5ns, identified from their stable energy graphs.The root mean square deviation (RMSD) of each trajectory with respective to its reference was found to be appropriate. Initially, parameters like temperature, density and energies were calculated in order to check the system equilibration. Temperature of all system was found to be stable at 300 K with fluctuation rate of ±2 K, however, density was lie between the ranges of 1.035-1.045 Kg/m^3. Moreover, kinetic, potential as well as their total energies did not show considerable fluctuation throughout the simulations, ensuring the structural consistency of biological system with simulated model. Later, root mean square deviation (RMSD), root mean square fluctuation (RMSF), hydrogen bonding and their angles occupancy rate analysis was also used to evaluate the difference of apo and complex structures of related proteins. Stability of all systems confirmed that the simulation length is sufficientto explore hidden information.

The RMSD of the protein backbone with reference to its initial structure is the measure of protein stability during simulation. Frequent comparison of subsequent structures showed the level of variation during the MD simulation through RMSD.Thus, 50ns simulations of two homologues with five known inhibitors ensured their stability in their complexes with low RMSDs, shown in figure-**4**. Apo-NEP (aNEP) and NEP2 (ahNEP2) were found to be more fluctuating than their respective complexes (figure-**5a**)indicating that the free hotspot residues are susceptible for high conformational changes than their bound forms. However, the chemistry of inhibitors also dictated the range of variations in protein-ligand complex under physiological conditions. Deviation of compound3 (cNEP, chNEP2), fasidotrilat

(fNEP, fhNEP2), omapatrilat (oNEP, ohNEP2), phosphoramidon (pNEP, phNEP2) and thiorphan (tNEP, thNEP2) from their original orientation within hNEP and hNEP2 presented structural transitions in the ranges of 1.6-2.0 Å, 1.7-2.0 Å , 1.6-1.7 Å, 1.6-2.0 Å, 1.75-2.2 Å and 2.0-2.6 Å, 1.5-2.25 Å, 1.6-2.25 Å, 1.5-2.0 Å, 1.75-2.2 Å, respectively. Apo protein to its binary transition allowed the rearrangement of hotspot residues with appropriate accommodation of ligand within it and helped to identify the inhibitory potency and specificity towards particular targets.Compound3 and omapatrilat are two inhibitors, upon complexation with hNEP and hNEP2, account for significant fluctuation resulted in huge differences in RMSDs, presented in figure-**5b-f**.Thus, the rate of ligand promoted conformational changesaffected their binding affinities to their receptors. These binding affinities and their strengths indirectly defined the therapeutic activities of these molecules.Similar pattern of RMSD indicated similar conformational changes in template and modeled proteins. However, residual fluctuation was observed to be very high in inhibitors bound form of both homologuesthan their respective apo forms.Particularly, omapatrilat upon complexation with hNEP2 showed high degree of residual fluctuation than others. Moreover, compound3 and thiorphan were found to be least fluctuating within the homologues, indicating their importance towards specific activity (figure-**6**). Human NEP2 was found to be more flexible than hNEP in all complexes, displayed increase RMSDs and RMSFs (figure-**5**&**6**),might be the reason for comparatively larger pocket size. B-factor, listed in table-**2**, another measure of fluctuating residues was calculated for both proteins with all inhibitors and found to be comparable with their interaction patterns and hydrogen bonding. In our simulations, B-factors underestimated the inhibitory potency of thiorphan with NEP2protein; however, hydrogen bond occupancy favored the molecule.

The above parameters ensured the system stability for further predictions.However, RMSF and B-factor also helped to explore the residual sides that underwent high conformational changes during simulation. Moreover, the regions that experienced huge alteration in their 3D orientations were found to have an active site and stabilized upon complex formation. Here, hydrogen bonds were divided into three categories for ease of analysis; no interactions (below 40% occupancy), weak interactions (between 40-60% occupancy) and strong interactions (above 75% occupancy), therefore, interactions below 40% were considered, here, as temporary or occasional. For real time analysis of protein dynamics, average protein

structures (pdbs) of each system at different intervalwere generated and used to compare the succeeding with precedingconfirmation. This is to identify the actual time after which the interaction become weak as a result ligand detached from its binding pocket. The analysis required the proper structural sampling from 500 different conformations generated from a production run of 50ns.

Due to the deficient structural information within the reference structure the residual numbering is different; however, the reference (1DMT) pdb's equivalent numbers to NEP and hNEP2 are listed in table-**1**. Moreover, table-**3** and figure-**3**displayed the interaction information for all ligands with both proteins for their comparison. Compound3 when complexed with hNEP and hNEP2 protein,displayed comparable B-factor (30.5319 & 31.01836, respectively), indicating similar fluctuation pattern with small difference in interaction affinities. NEP showed strong hydrogen bond interactions towards compound3 through bidentate Arg664 with occupancy rate of 96.56% and 99.29%. Beside this, few occasional hydrogen bonds were also observedwith low percent occupancylikewith Asn489 (9.8%), Val488 (7.09%), Glu531 (39.79%) and Glu593 (30%). Interactions with low persistence rate are not important in binding rather they support the ligand's accommodation within its active site. Before simulation, amide oxygen, carboxylate oxygen and pyrrole nitrogen of compound3 were found to be crucial for interactions in both proteins (presented in figure-**3**). However, after simulation, chNEP2 showed very few interactions with the active site residues as compared to the cNEP complex. From the above interaction patterns and conformational alterations, depicted in figure-**7**, it is observed that the catalytic Arg664 and Glu531of hNEP are stable in their initial conformations throughout the simulation. The conformational stability and consistent interactions of Arg664 and Glu531 allowed the inhibitor (compound3)to attain the stability to block the protein induced hydrolysis. While the two residues, Arg661 and Glu528, in the hNEP2 were stable only for initial 30ns simulations. However, they changed their conformations,frequently, from non-extended to extended form after this initial period of stability. This conformational variation might be the reason of larger pocket site, in which ligand was continuously tried to acquire appropriate position to maintain interactions within protein.

Similarly, fasidotrilat interacted, comparatively, with more consistent bidentate hydrogen

bonding with Arg664 and monodentate hydrogen bonding with His658 of hNEP that was found to be comparatively weak for the hNEP2 protein. The extended conformation of inhibitor in hNEP2 pocket might be the reason of its weak interactions. However, interaction with Asn486 in fhNEP2 is stronger (73.57%) than fNEP (0.61%) with more consistent bond formation and less frequent fluctuation throughout the simulation. Figure-**3** and **8**displayed docked conformations and hydrogen bond graphsof fasidotrilat within two proteins, respectively. Total evaluation of interactions and their occupancy rates showed that the interactionswith NEP protein are consistent before and after simulations; however, NEP2 left the ligand with huge conformational changes after constant interactionstill 30ns. Moreover, Asn486 maintained the interaction with ligand up till 40ns simulations.Due to these hydrogen bond formation and destruction throughout simulation of fhNEP2, fasidotrilat is considered as strong binder for hNEP than hNEP2, suggested by their inhibitory concentrations as well. Fasidotrilat with K_i value of 5nM[27] and more consistent interactions with hNEP were considered to be more specific for peripheral effects then cerebral; however, strong interactions of shorter half-lives and 16nM[27] inhibitory concentration against hNEP2 showed it non-selective nature.

Omapatrilat with 3nM and 8nM[27] inhibitory activities for human NEP and NEP2 homologues again showed the non-selective nature of molecule with little differences. Initially, ligand showed huge conformational variation, indicating the molecular flexibility with bulkier group. Starting 10ns were required by the ligand to attain proper orientation for interaction, after that the stable consistent interactions were observed.However, the appropriate distance with catalytic Glutamate is more promising in hNEP2, rather, fluctuating in NEP. Arg664/661 and Glu531/528 residues were involved in establishing stable hydrogen bond with inhibitor in both proteins, as depicted in figure-**9**. Further, molecule do not show considerable difference among the inhibitory activity and interaction pattern of two proteins to be selective for particular homologues.

Phosphoramidon, a cognate ligand of reference crystal structure[29], preserved all reported interactions with active site residues of hNEP, presented in figure-**3**. However, in pocket site of hNEP and hNEP2, over 10 ns of simulation, it lost interactions with Asn489/486 (23.19 and 12.05%), Val488/485 (15.4 and 44.48%) and Ala490/487 (2.32%) due to their highly

flexible state. Moreover, figure-**10** showed ligand's strong, consistent interactions with Arg664, Glu531 and His658 of hNEP proved it as more efficient anti-hNEP agent than hNEP2. Number of hydrogen bonds throughout simulations was observed to be more in case of NEP, furthermore, its inhibitory activity (0.8nM)[27]is also better for hNEP, might be due to easily accessible pocket site for inhibitors. Hydrophobic interactions and ligand's orientation could also play an efficient role to support good phosphoramidon's inhibitory activity towards hNEP.

Contrary, thiorphan in hNEP2 interacted with good binding potentials towards one site of its binding pocket, however, its inhibitory concentration was found to be better for hNEP. Arg661 and Glu528 showed good persistent hydrogen bond occupancy in hNEP2 protein whereas Arg664 of hNEP mediated a weak interaction towards thiorphan (figure-**11**). Ligand obtained flexible conformation within hNEP2's active site due to which only Arg661, mediated hydrogen bonds, bound the ligand throughout the simulation. However, catalytic His655 and Glu528 couldn't take part in ligand binding, required to maintain the suitable distance with Zn and catalytic residues. Thus, improper ligand orientations within active site of NEP2 protein weakenits binding potential. However, Glu531 in NEP played prominent role to hold the ligand within appropriate position for its activity.Though, the bidentate interactions of Arg664 were not favorable, even then tried the ligand to keep in close proximity for its activity.Here, we didn't include any constrain in our simulation to resemble the blood brain barrier (BBB), computationally. Thus, direct thiorphan binding to hNEP2 without physiologicalrestrictionmight be the reason of its strong binding.

Overall analysis indicated that the loss of hydrogen bonding mediated from Arg664/661 at any stage of simulation made inhibitors less potential against NEP/NEP2. This is because, high affinity interaction with this residual site was observed in all complexes of NEP except with thiorphan. However, Arg49 and Glu531, in tNEP maintained the complex stability when bidentate bonds of Arg664 broken to ensure its activity against NEP.Moreover, conformational stability and ligand's orientation is favorable in all cases; however, compound3, fasidotrilat, omapatrilat and phosphoramidon are more effective towards NEP with no selectivity. Little more concentrations of these inhibitors block the cerebral activity of NEP related protein due to similar pattern of interaction and dynamic behavior of these

molecules. Although, thiorphan with larger inhibitory concentration (4nM for NEP and 120nM for NEP2)[27] and small size, showed drastic conformational changes upon simulation. Thus, restrict the cerebral activity of molecule and predicted to be peripheral selective blocker of NEP.

3. METHODOLOGY:

To explore the structural requirement for designing target antagonist, crystallographic protein data is required. In our case, related data is not available that flourished by *in-silico* homology modeling. In the physiological environment, protein alone or drug binding to it is a dynamic process. This identification is not easy because whenever a small molecule approaches a protein, protein undergo huge conformational changes for its accommodation inside the space available. Exploration of neprilysin interaction pattern with its inhibitors to know hidden key points for development of more targeted molecule for peripheral receptor that have no or little cerebral effects was conducted with homology modeling and dynamic simulation.

3.1. Homology Modeling:

Molecular homology modeling required a target along with its template sequence for the spatial hNEP2 structure, downloaded from NCBI database[36]. Accession number Q495T6 was downloaded for hNEP2 modeling, followed by template inquiring *via* Blast search[37]. NEP with pdb code 1DMT[38] was identified as most appropriate reference structure with high degree alignment for NEP2 modeling. Molecular Operating Environment (MOE)[39] modeling tool was used to build NEP2 structure coordinates from 3D information of NEP protein. Initially, ten different models were generated that were then evaluated for their residual packing quality and appropriately stable energy. However, starting 86 residues of hNEP2 couldn't model due to lack of their structural information in NEP protein and not included in our final selected model.

Geometrical strains were allowed to remove through minimization and finally, zinccoordinates were transferred to refined model, manually. PROCHECK[40] and Ramachandran plot[41] were used to rectify the stereochemical and geometrical errors within

modeled structure, respectively. Selected and validated model was preserved as ahNEP2, the apo form of human NEP2 protein. hNEP2 complexes with five reported NEP inhibitors (compound3, fasodotrilat, omapatrilat, phosphoramidon and thiorphan) were constructed using docking tool of MOE. Docking simulation of these compounds within hNEP2 active site, identified via its superimposition on NEP crystal structure, resulted it five complex structures along with an apo form. Ligands were prepared by protonation, addition of charges and minimization for their docking to the hNEP2 protein through GOLD[42], a genetic algorithm based docking software. The best docked pose of each inhibitor in complex form were save as chNEP2, fhNEP2, ohNEP2, phNEP2 and thNEP2 along with reference cNEP, fNEP, oNEP, pNEP and tNEP for comparison.

3.2. Protein Dynamic Scaling:

Human NEP, predominantly found in peripheral tissues, used to model hNEP2 having high degree sequence similarity. hNEP2, another important member of neprilysin family, is localized in central nervous system and testis to regulate reproduction. Modeled hNEP2 with or without inhibitors were used here to explore their dynamics. Total twelve systems were used that symbolized as aNEP (apo NEP protein), cNEP (NEP with compound3), fNEP (NEP with fasodotrilat), oNEP (NEP with omapatrilat), pNEP (NEP with phosphoramidon), and tNEP (NEP with thiorphan), with modeled ahNEP2 (apo hNEP2 protein), chNEP2 (hNEP2 with compound3), fhNEP2 (hNEP2 with fasodotrilat), ohNEP2 (hNEP2 with omapatrilat), phNEP2 (hNEP2 with phosphoramidon), and thNEP2 (hNEP2 with thiorphan). These systems were energy minimized individually using Amber99[43] in order to remove geometrical strains and obtained optimally stable conformation. Electrostatic potential charges on ligands were assigned using Gaussian03[44] followed by its parametrization using antechamber module in Amber10[45]. Recognition parameters for Zn geometry are missing in Amber, however, CaDA (Cationic Dummy Atom) approach was applied for its loading[46]. This approach resulted in generation of four dummy atoms having evenly distributed charges of Zn, helped to satisfy Zn's octahedral geometry within protein. Lastly, systems were equalized to the natural system through solvate it with TIP3P cubic box of 8Å and neutralized with positive ions followed by generation of prmtop (topology) and inpcrd (coordinates) files using xleap. Sander, module incorporated in Amber, was used for

minimization, equilibration and MD simulation.

In xleap, Generalized Amber Force Field (gaff)[47] and Duan Force Field parameters were used to deal with inhibitors and protein, respectively. Step wise minimization (gradual unrestraining system) of whole structure was conducted to obtained stable converge models. Following the minimization, systems were gradually heated from 0 to 300 K to achieve ambient temperature over 50 ps. Constant temperature and pressure of 300 K and 1 atmosphere was used to run MD simulations. Atoms involved in hydrogen bonding and electrostatic interactions were allowed to preserve in their position by application of SHAKE[48]and Particle Mesh Ewald method[49]. Point of system stability was identified via equilibration that expands through 2 fs time step simulations of 50 ns. Finally, simulation analysis of generated data was done using PTRAJ[50]. System energies, temperatures and densities along with hydrogen bond occupancy rates, their distances and angles were used to explore their interacting behavior.

4. CONCLUSION:

The informational gap in neprilysin and related targets to establish selective blocker motivate us to model hNEP2 structure. Inhibitors that showed specificity for NEP were considered to be less effective for inhibition of protective cerebral effect of hNEP2. Homology modeling of hNEP2 from NEP resulted a validated secondary structure thatfurther used to generate five different complexes. These five complexes for each protein were manually evaluated for their interaction and finally, subjected for molecular dynamic simulations to obtained a clear picture of their affinities. Simulation of complex structures revealed prominent fluctuation upon ligand binding than their unbound forms. However, conformational alterations were found to be more in hNEP2 than NEP protein. Active site Arg and Glu along with Zn showed their valuable role in substrate or inhibitor binding. Compound3 and omapatrilat were obtained with similar conformations. However, hNEP allowed them to interact more effectively with hNEP2, due to its size difference. Nevertheless, phosphoramidon with slightly change conformation made it quite selective for hNEP protein. The experimental and theoretical results were wellcorrelated.The ligand fitted itself with similar orientation in two proteins and showed better predicted inhibition for

hNEP2. Thus, small sized inhibitors like thiorphan, the Arg49 and Arg664 are found to be interactive to support the ligand binding in NEP while only Arg661 is solely interactive in NEP2. The two side interacting capability of NEP allowed the ligand to settle more effectively. However, in NEP2 due to larger pocket, small ligand is unable to capture both sites.Thus, larger pocket size might be responsible for lower inhibitory activity of thNEP2. Structural features of two proteins with five inhibitors and their dynamics render undiscovered knowledge that might be useful to design selective inhibitors of NEP and hNEP2.

ACKNOWLEDGEMENT:

Financial support for the establishment of Cluster Computer at the PCMD from HigherEducation Commission, Pakistan is highly acknowledged. The authors are also grateful to the AMBER supporting team for providing us AMBER software free of cost.

CONFLICT OF INTEREST:

There is no conflict of interest among the authors.

REFERENCES:

1. Malfroy, B., Kuang, W. J., Seeburg, P. H., Mason, A. J. and Schofield, P. R. (1988) Molecular cloning and amino acid sequence of human enkephalinase (neutral endopeptidase). FEBS Lett. *229*, 206-210
2. Galia, G.; Andrea, F. R.; Melanie, C.; Mieczyslaw, M.; Nabil, G. S.; Philippe, C.; Desgroseillers, L.; Boileau, G. Molecular cloning and Biochemical Characterization of a new mouse testis soluble-zinc-metallopeptidase of the neprilysin family. *J. Biochem. Soc.***2000**, *347*, 419-429.
3. Xu, D., Emoto, N., Giaid, A., Slaughter, C., Kaw, S., DeWit, D. and Yanagisawa, M. (1994) ECE-1 : a membrane-bound metalloprotease that catalyzes the proteolytic activation of big endothelin-1. Cell *78*, 473-485.
4. Emoto, N. and Yanagisawa, M. (1995) Endothelin-converting enzyme-2 is a membrane-bound, phosphoramidon-sensitive metalloprotease with acidic pH optimum. J. Biol. Chem. *270*, 15262-15268.
5. Valdenaire, O., Richards, J. G., Faull, R. L. and Schweizer, A. (1999) XCE, a new member of the endothelin-converting enzyme and neutral endopeptidase family, is preferentially expressed in the CNS. Mol. Brain Res. *64*, 211-221.
6. Soohee, Lee.; Asim, K. D.; Colvin M. R. Active amino acids of the Kell blood group protein and model of the ectodomain based on the structure of neutral endopeptidase 24.11. *Blood*.**2003**, *102*, 3028-3034.
7. Du, L., Desbarats, M., Viel, J., Glorieux, F. H., Cawthorn, C. and Ecarot, B. (1996) cDNA cloning of the murine *Pex* gene implicated in X-linked hypophosphatemia and evidence for expression in bone. Genomics *36*, 22-28.
8. Marr, R. A.; Spencer, B. J. Diabetes NEP-like Endopeptidases and Alzheimer's Disease, *Curr. Alzh. Res.***2010**, *7*, 223-229.
9. Turner, A.J. and Tanzawa, K. (1997) Mammalian membrane metallopeptidases: NEP, ECE, KELL, and PEX. Faseb J. 11, 355–364.
10. Christian, O.; Bernard P. R.; Marie-Claude F. Z.; Glenn E. D. Structural analysis of neprilysin with various specific and potent inhibitors. *ActaCrystallogr., Sect. D: Biol. Crystallogr.***2004**, *D60*, 392-396.
11. Gillian, I. R.; Amy, L. J.; Peter, J. G.; Angela, M. C.; Anthony, J. T.; Nigel, M. H.

Circulating Activities of Angiotensin- Converting Enzyme, Its Homology, Angiotensin- Converting Enzyme 2, and Neprilysin in a Family Study. *Hypertension, J. Am. Heart Assoc.***2006**, *48*, 914-920.

12. Nikolaos, D.; Athanasios, P.; Georgios, A. D.; Edward, D. S.; Georgios, A. S. A Computational Approach to the Study of Binding Mode of Dual ACE/ NEP Inhibitors. *J. Chem. Inf. Model.***2010**, *50*, 388-396.
13. Standeven, K. F.; Hess, K.; Carter, A. M.; Rice, G. I.; Cordell, P. A.; Balmforth, A. J.; Lu, B.; Scott, D. J.; Turner, A. J.; Hooper N. M.; Grant, P. J. Neprilysin, obesity and the metabolic syndrome, *Int. J. Obes.***2011**, *35*, 1031-1040.
14. Ottaviani, E.; Malagoli, D.; Grimaldi, A.; de Eguileor, M. The immuneregulator role of neprilysin (NEP) in invertebrates. *Minireview*, **2012**, *9*, 207-211.
15. Bralet, J., and Schwartz, J.-C. (2001). Vasopeptidase inhibitors: An emerging class of cardiovasculardrugs. Trends Pharmacol. Sci. 22, 106–109.
16. Francisco, M. P.; Cristina, G. R.; Nerea, S.; Antonio, Cejudo-Roman.; Manuel, Fernandez-Sanchez.; Jon, Irazusta.; Nicolas, G.; Luz, Candenas. Autocrine regulation of human sperm motility by tachykinins. *Reprod. Biol. Endocrinol.***2010**, *8(1)*, 104-113.
17. Sitnik, J. L.; Francis, C.; Hens, K.; Huybrechts, R.; Wolfner, M. F.; Callaerts, P. Neprilysins: an evolutionarily conserved family of metalloproteases that play important roles in reproduction in Drosophila. *Genetics*. **2014**, doi: 10.1534/genetics.113.160945.
18. Ikeda,K.,Emoto,N.,Raharjo,S.B.,Nurhantari,Y.,Saiki,K.,Yokoyama,M., etal.(1999).Molecularidentificationandcharacterizationofnovelmembrane-boundmetalloprotease,thesolublesecretedformofwhichhydrolyzesavarietyofvasoactivepeptides. *J. Biol.Chem.* 274, 32469–32477.doi:10.1074/jbc.274.45. 32469
19. Ghaddar,G.,Ruchon,A.F.,Carpentier,M.,Marcinkiewicz,M.,Seidah,N.G., Crine,P.,etal.(2000).Molecularcloningandbiochemicalcharacterization ofanewmousetestissoluble-zinc-metallopeptidaseofthneprilysinfamily. *Biochem.J.* 347, 419–429.doi:10.1042/0264-6021:3470419
20. Bonvouloir,N.,Lemieux,N.,Crine,P.,Boileau,G.,andDesGroseillers,L. (2001). Molecularcloning,tissuedistributionandchromosomallocalizationofMMEL2,agenecod

ingforanovelhumanmemberoftheneutralendopeptidase-24.11family. *DNACellBiol.*20, 493–498.doi:10. 1089/104454901316976127

21. Me´lanie Carpentier,1 Christine Guillemette,2 Janice L. Bailey,2 Guy Boileau,1 Lucie Jeannotte,3 Luc DesGroseillers,1,4†*and Jean Charron3† Reduced Fertility in Male Mice Deficient in the Zinc Metallopeptidase NL1. MOLECULAR AND CELLULAR BIOLOGY, May 2004, p. 4428–4437.
22. Alison R. Whyteside, Anthony J. Turner, Human neprilysin-2 (NEP2) and NEP display distinct subcellular localisations and substrate preferences. FEBS Letters 582 (2008) 2382–2386.
23. Robert A. Marr * and Daniel M. Hafez,Amyloid-beta and Alzheimer's disease: the role of neprilysin-2 in amyloid-beta clearance, Frontiers in Aging Neuroscience2014, Volume 6, Article 187. doi: 10.3389/fnagi.2014.00187.
24. N. N. Nalivaeva,1, 2 N. D. Belyaev,1 I. A. Zhuravin,2 and A. J. Turner1, The Alzheimer's Amyloid-Degrading Peptidase, Neprilysin: Can We Control It? International Journal of Alzheimer's Disease Volume 2012, Article ID 383796, 12 pages.doi:10.1155/2012/383796
25. Daniel, H.; Jeffrey, Y. H.; Alexis, M. H.; Stephanie, V.; Edward, R.; Angela, M. B.; Bao, Lu.; Luc, DesGroseillers.; Eliezer, M.; Robert, A. M. Neprilysin-2 is an important β-Amyloid Degrading Enzyme. *The Am. J. Pathol.***2011**, *178(1)*, 306-312.
26. Shirotani,K.,Tsubuki,S.,Iwata,N.,Takaki,Y.,Harigaya,W.,Maruyama,K., etal.(2001).Neprilysindegradesbothamyloidbetapeptides1–40and1-42 most rapidlyandefficientlyamongthiorphan-andphosphoramidon-sensitive endopeptidases. *J. Biol.Chem.* 276, 21895–21901.doi:10.1074/jbc.m008511200.
27. Christiane ROSE, Ste! phanie VOISIN, Claude GROS, Jean-Charles SCHWARTZ and Tanja OUIMET. *Cell-specific activity of neprilysin 2 isoforms and enzymic specificity compared with neprilysin* Biochem. J. (2002) *363*, 697-705.
28. Voisin, S., Rognan, D., Gros, C., and Ouimet, T. (2004). A three-dimensional model of the neprilysin2 active site based on the X-ray structure of neprilysin. Identification of residues involved in substrate hydrolysis and inhibitor binding of neprilysin2. *J. Biol.Chem.* 279, 46172–46181.doi:10.1074/jbc.m407333200
29. Christian, O.; Allan, D'Arcy.; Michael, H.; Fritz, K. W.; Glenn, E. D. Structure of

Human Neutral Endopeptidase (Neprilysin) complexed with Phosphoramidon. *J. Mol. Biol.***2000**, *296*, 341-349.

30. Alison, R. W.; Anthony, J. T. Human neprilysin-2 (NEP2) and NEP display distinct subcellular localizations and substrate preferences. *FEBS Lett.***2008**, *582*, 2382-2386.
31. Soohee, Lee.; Asim, K. D.; Colvin, M. R. Active amino acids of the Kell blood group protein and model of the ectodomain based on the structure of neutral endopeptidase 24.11. *Blood*, **2003**, *102*, 3028-3034.
32. Roger, S. H. Evolution of Mammalian KELL Blood Group Glycoproteins and Genes (KEL): Evidence for a Marsupial Origin from an Ancestral M13 type II Endopeptidase Gene. *J. Phylogene. Evol. Biol.***2013**, *1*, 111-119.
33. Zaheer, Ul-Haq.; Sadaf, I.; Syed, T. M. Dynamic changes in the secondary structure of ECE-1 and XCE account for their different substrate specificities. *BMC Bioinformatics*. **2012**, *13*, 285-299.
34. Khatuna, G.; Sachchidanand; Raphael, R.; Mihaly, M.; Ming-Ming, Z.; Lakshmi, A. D. Homology Modeling and Site-Directed Mutagenesis to identify Selective Inhibitors of Endothelin-Converting Enzyme-2. *J. Med. Chem.***2008**, *51*, 3378-3387.
35. Josie, E. T.; Caroline, M. R.; Ahmet, C.; Nicholas, D. B.; Richard, J. B.; Alan, D. S.; Anthony, J. T.; Elwyn, R. I. *Drosophila Melanogaster* NEP2 is a new soluble member of the neprilysin family of endopeptidases with implications for reproduction and renal function. *J. Biochem. Soc.***2005**, *386*, 357-366.
36. Geer, L. Y.; Marchler-Bauer, A.; Geer, R. C.; Han, L.; He, J.; He, S.; Liu, C.; Shi, W.; Bryant, S. H. The NCBI BioSystems database. *Nucleic Acids Res.***2010**, *38*, D492-496. [PubMed PMID: 19854944]
37. Altschul, S.F.; Gish, W.; Miller, W.; Myers, E.W.;Lipman, D.J. Basic local alignment search tool.*J. Mol. Biol.***1990**, *215*, 403-410.
38. Oefner, C.; D'Arcy, A.; Hennig, M.; Winkler, F. K.; Dale, G. E. Structure of human neutral endopeptidase (Neprilysin) complexed with phosphoramidon. *J. Mol. Biol.***2000**, *296*, 341-349, DOI: 10.1006/jmbi.1999.3492.
39. Molecular Operating Environment (MOE), 2013.08; Chemical Computing Group Inc., 1010 Sherbooke St. West, Suite #910, Montreal, QC, Canada, H3A 2R7, **2013**.

40. Laskowski, R. A.; Macarthur, M. W.; Moss, D. S.; Thornton, J. M. PROCHECK: a program to check the stereochemical quality of protein structures, *J. Appl. Cryst.*, **1993**, *26*, 283-291.
41. Ramachandran, G.N.; Ramakrishnan, C.; Sasisekharan, V.Stereochemistry of polypeptide chain configurations.*J. Mol. Biol.***1963**, *7*,95–9, DOI:10.1016/S0022-2836(63)80023-6.
42. Jones, G.; Willett, P.; Glen,R. C. Molecular recognition of receptor sites using a genetic algorithm with a description of desolvation.*J. Mol. Biol.***1995**, *245*, 43-53,DOI: 10.1016/S0022-2836(95)80037-9
43. Wang, J.; Wolf, R. M.; Caldwell, J. W.;Kollman, P. A.; Case, D. A. Development and testing of a general AMBER force field.*J. Comput. Chem.***2004**, *25*, 1157-1174.
44. Frisch, M. J.; Trucks, G. W.; Schlegel, H. B.; Scuseria, G. E.; Robb, M. A.; Cheeseman, J. R.; Scalmani, G.; Barone, V.; Mennucci, B.; Petersson, G. A. Gaussian 09, revision A. 02, Wallingford: Gaussian. Inc; **2009**.
45. Case, D. A III.; Cheatham, T. E III.; Darden, T.; Gohlke, H.; Luo, R.; Merz, K.; M Jr, Onufriev, A.; Simmerling, C.; Wang, B.; Woods, R. J. The Amber biomolecular simulation programs. *J. Comput. Chem.***2005**, *26*, 1668-1688.
46. Pang, Y. P. Novel zinc protein molecular dynamics simulations: Steps toward antiangiogenesis for cancer treatment. *J. Mol. Model.***1999**, *5*, 196-202.
47. Wang, J.; Wolf, R. M.; Caldwell, J. W.;Kollman, P. A.; Case, D. A. Development and testing of a general amber force field. *J.Comput. Chem.***2004**, *25*, 1157-1174.
48. Miyamoto, S.;Kollman, P. A. SETTLE: an analytical version of thr SHAKE and RATTLE algorithm for rigid water models. *J.Comput. Chem.***1992**, *13*, 952-962.
49. Darden, T.; York, D.; Pedersen, L. Particle mesh Ewald: An N log (N) method for Ewald sums in large systems. *J. Chem. Phys.***1993**, *98*, 10089-10092.
50. Daniel, R. R.; Thomas, E. C. PTRAJ and CPPTRAJ: Software for Processing and Analysis of Molecular Dynamics Trajectory Data. *J. Chem. Theory Comput*.**2013**, DOI:10.1021/ct400341p.

Table-**1**: Equivalent residual numbering of NEP and NEP2 proteins with reference (1DMT) structure residues.

Residues	**1DMT**	**NEP**	**NEP2**
Zn	Zn755	Zn697	Zn694
Arg	Arg717	Arg664	Arg661
Asn	Asn542	Asn489	Asn486
Glu	Glu584	Glu531	Glu528
Glu	Glu646	Glu593	Glu590
Val	Val541	Val488	Val485
His	His711	His658	His655
Arg	Arg102	Arg57	Arg57
Arg	Arg110	Arg49	Arg49
Ala	Ala543	Ala490	Ala487
Tyr	Tyr545	Tyr492	Tyr489

Table-**2**: Values of B-factor for both NEP and NEP2 proteins with all subjected compounds for comparative interaction capability within two proteins.

	hNEP	**hNEP2**
Apo	36.2297	32.5745
Complex with Compound3	30.5319	31.0184
Complex with Fasodotrilat	25.5834	36.2883
Complex with Omapatrilat	33.2025	49.8478
Complex with Phosphoramidon	27.1312	29.9795
Complex with Thiorphan	24.7157	28.26036

Table-**3**: Potential interactions and binding affinity of all ligands with two related proteins.

Complex	Zn697/ 694	Arg664/ 661	Asn489/ 486	Glu531/ 528	Glu593/5 90	Val488/ 485	His655/6 58	Arg57	Arg49	Ala490	Tyr492
cNEP	S1..D4 100%	O..HH12 99.29%	O..HD21 9.8%	S1..HE2 39.79%	S1..OE1 30%	H17..O 7.09%	-	-	-	-	-
	-	O..HH22 96.56%	-	-	-	-	-	-	-	-	-
fNEP	S1..D4 100%	O4..HH12 90.18%	O..HD22 0.61%	-	-	-	S1..HE2 66.67%	-	-	-	-
	-	O4..HH22 83.87%	S1..HD21 0.06%	-	-	-	-	-	-	-	-
oNEP	S1..D4 100%	O..HH12 82.00%	-	S1..HE2 66.16%	-	-	-	O3..HH12 35.2%	O2..HH12 6.97%	-	-
	-	O..HH22 77.77%	-	-	-	-	-	O3..HH22 19.71%	O2..HH22 8.62%	-	-
pNEP	O2P..D4 99.29%	O6..HH12 97.65%	H12..OD1 23.19%	O1..HE2 47.7%	O2P..OE1 40%	H17..O 15.4%	O1P..HE2 97.93%	-	-	H23..O 2.32%	O3..H 93.78%
	-	O6..HH22 94.13%	H1..OD1 11.82%	-	-	-	-	-	-	-	-
tNEP	S1..D4 100%	O2..HH12 52.05%	-	S1..HE2 89.32%	-	-	O..HD1 4.39%	-	O1..HH12 39.42%	-	-
	-	O2..HH22 30.57%	-	S1..OE1 87%	-	-	-	-	O1..HH22 33.68%	-	-

chNEP2	S1..D4 100%	O..HH12 63.75%	O2..HD21 4.8%	S1..HE2 60.26%	-	H17..O 6.73%	-	-	-	-	-
	-	O..HH22 54.15%	-	-	-	-	-	-	-	-	-
fhNEP2	S1..D1 100%	O4..HH12 57.38%	H5..OD1 73.57%	-	-	-	S1..HE2 3.24%	O..HH22 15.47%	-	-	-
	-	O4..HH22 49.72%	-	-	-	-	-	-	-	-	-
ohNEP2	S1..D4 100%	O..HH12 94.62%	O1..HD21 4.04%	S1..HE2 85.2%	-	-	Pyrrole.. HC	O2..HH12 38.67%	O3..HH12 27.2%	-	-
	-	O..HH22 88.72%	-	-	-	-	-	-	O3..HH22 28.9%	-	-
phNEP2	O1P..D4 99%	O6..HH12 86.93%	O0..HD21 12.05%	O2P..HE2 53.98%	-	H8..O 44.48%	O1P..HE1 57.78%	-	-	-	-
	-	O6..HH22 45.2%	H3..OD1 5.91%	-	-	-	-	-	-	-	-
thNEP2	S1..D4 100%	O2..HH12 94.2%	O..HD21 1.65%	S1..OE1 74.3%	-	-	-	-	O1..HH12 27.62%	-	-
	-	O2..HH22 94.6%	-	S1..HE2 74.34%	-	-	-	-	-	-	-

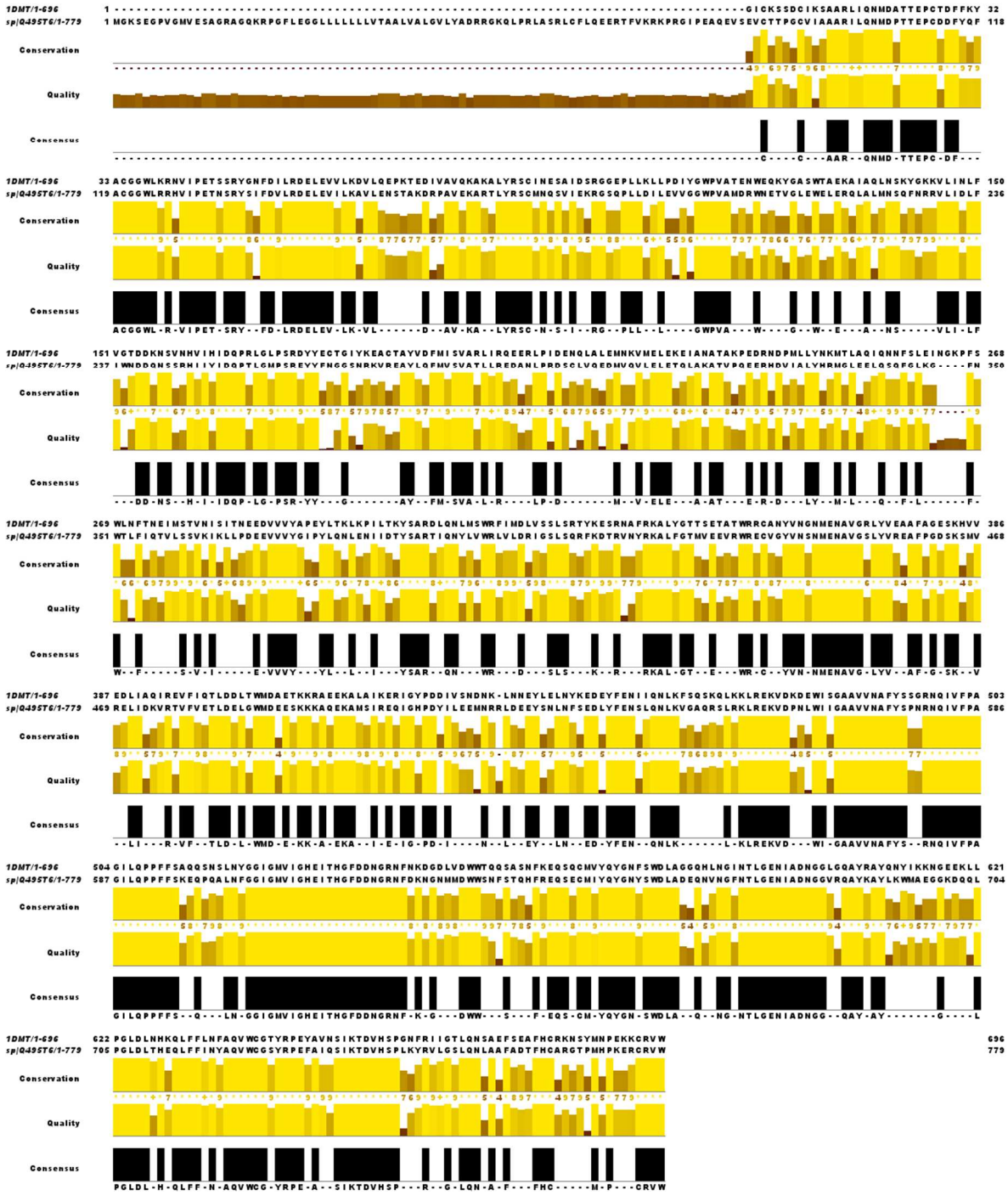

Figure-**1**: Sequence Alignment of hNEP2 upon NEP protein,through Jalview, showed high degree sequence similarity, proposing good structural similarity too.

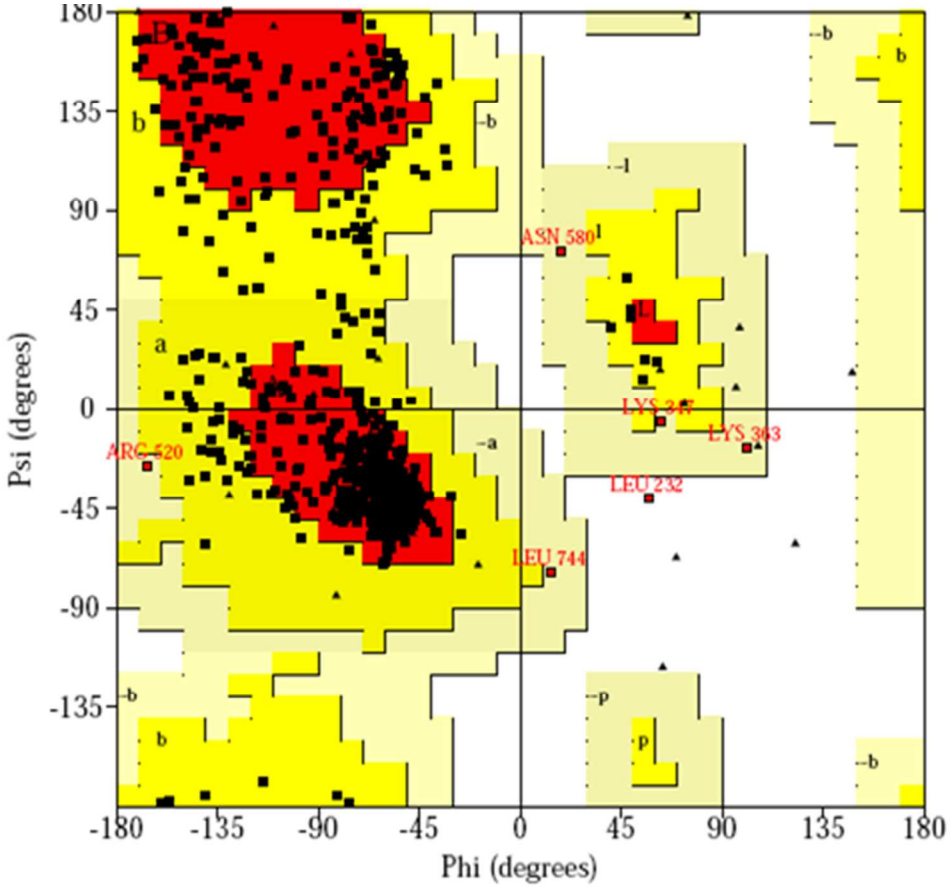

Figure-**2**: Correlation between Phi and Psi, used by Ramachandran plot, proved generated model authenticity with excellent residual percentage in allowed region and low to no percentages in additionally allowed and disallowed regions.

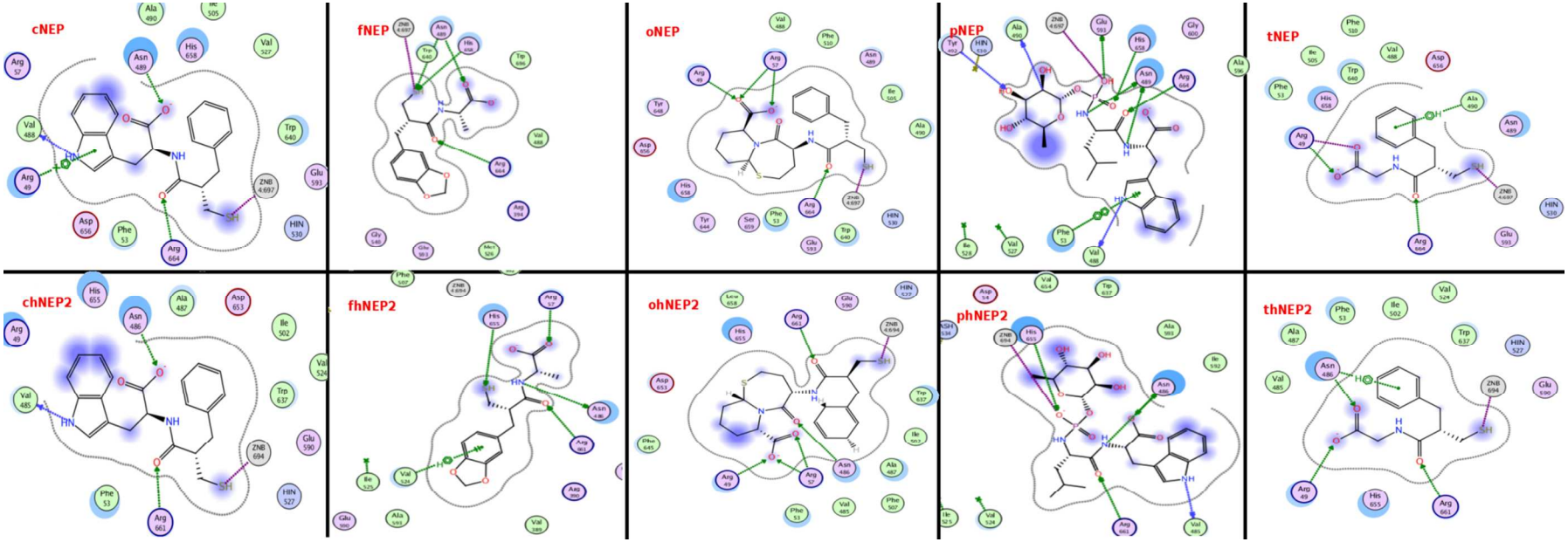

Figure-**3**: Interaction patterns of five inhibitors with NEP (upper panel) and hNEP2 (lower panel) showed involvement of same residues and ligand's moieties incomplex formation.

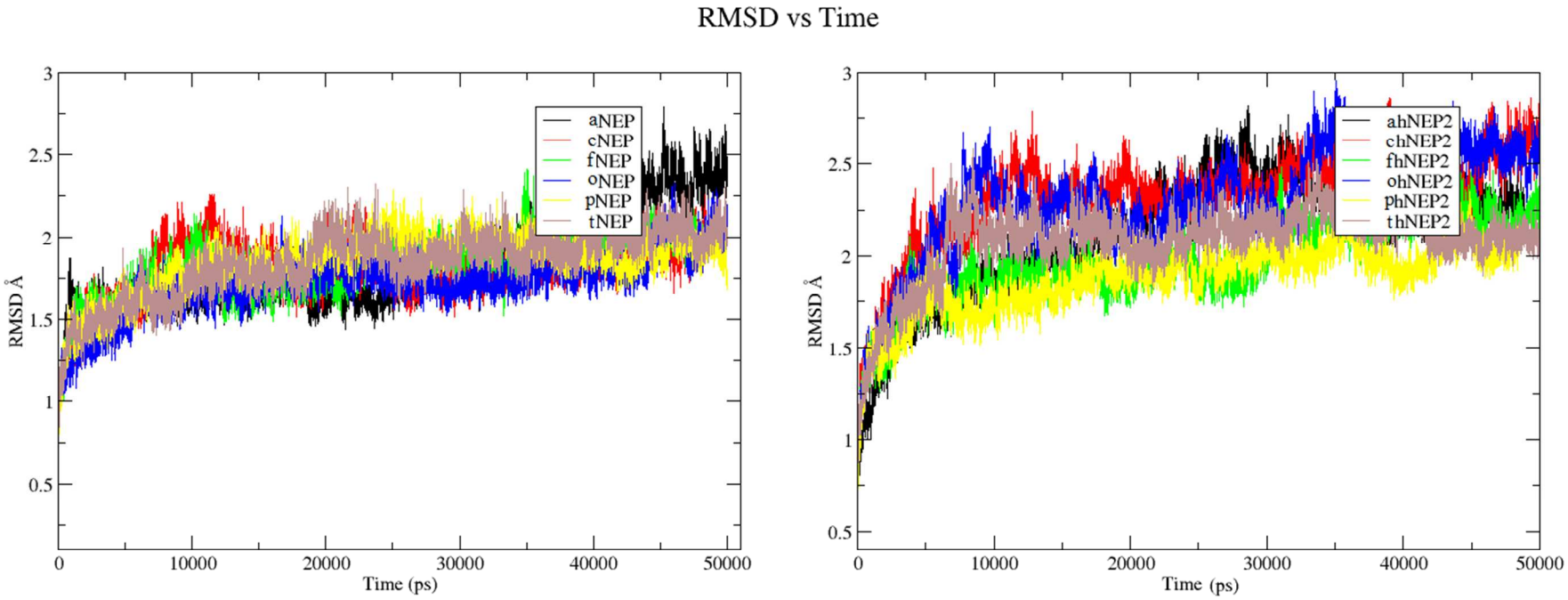

Figure-**4**: Backbone deviationof each coupled with its uncoupled protein over the period of 50ns showed system stability with less fluctuating RMSDs. Left and right panelsaredemonstrativeof NEP and hNEP2 proteins, respectively.

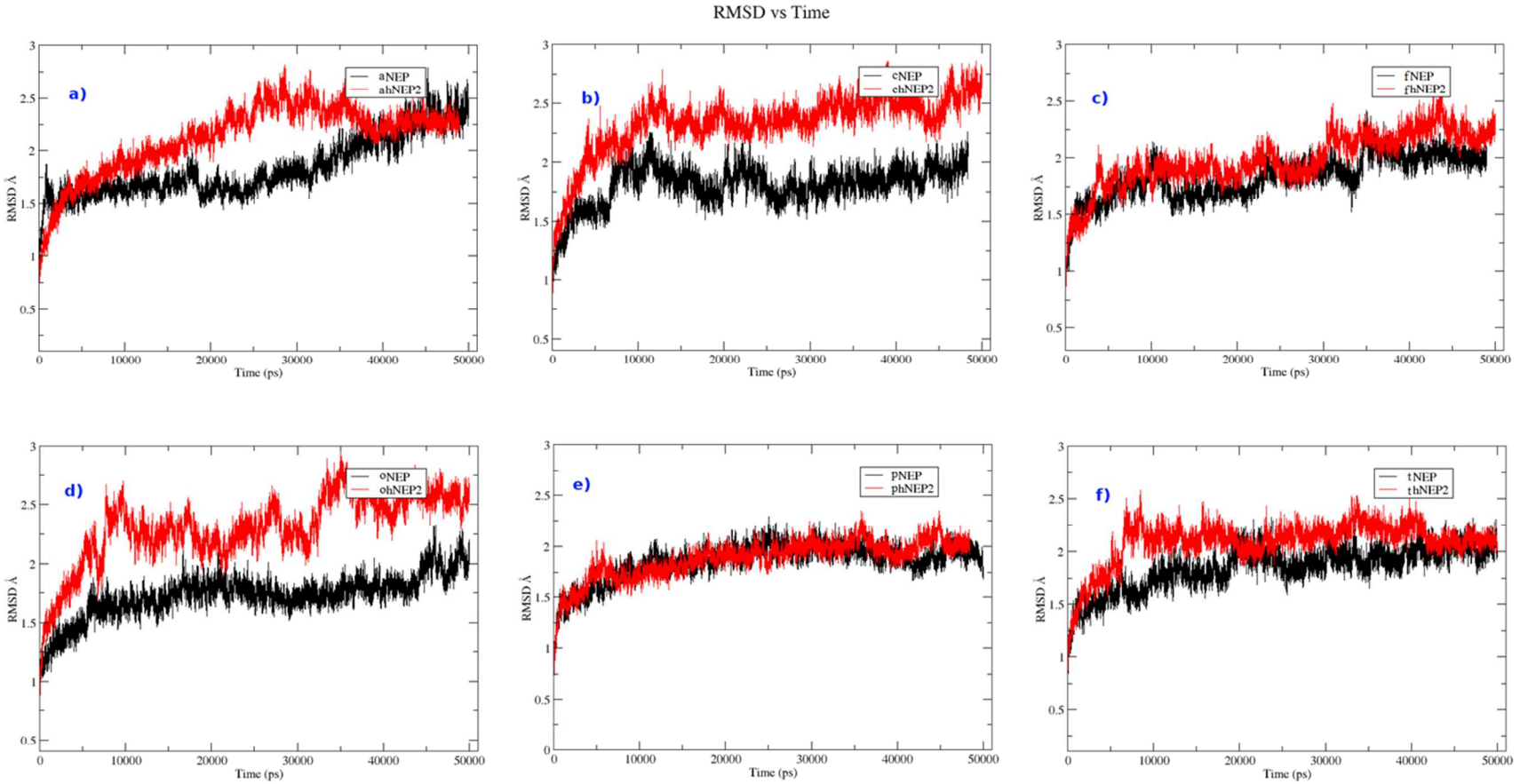

Figure-**5**: Backbone RMSDs of apo and each complex of hNEP2 with its respective reference. Apo proteins (a) were found to be more flexible than their complexes; however, NEP and hNEP2 were more fluctuating upon compound3 and omapatrilat (b & d) binding. Rate of backbone conformational change is same in both proteins for phosphoramidon (e), furthermore, fasidotrilat and thiorphan (c & f) showed low level of changes during simulation.

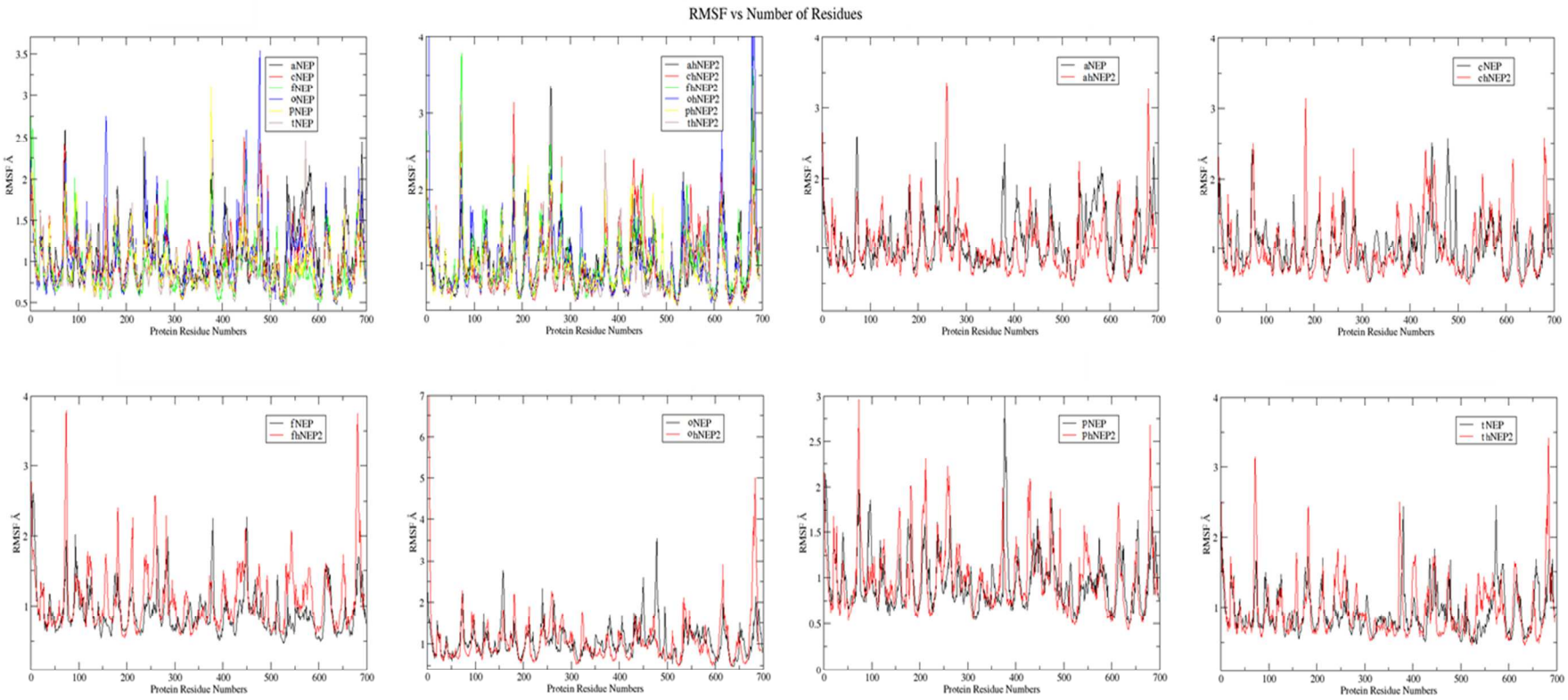

Figure-**6**: Root Mean Square Fluctuation of all systems over 50ns simulation, showed degree of residual fluctuation and their comparison with their references.

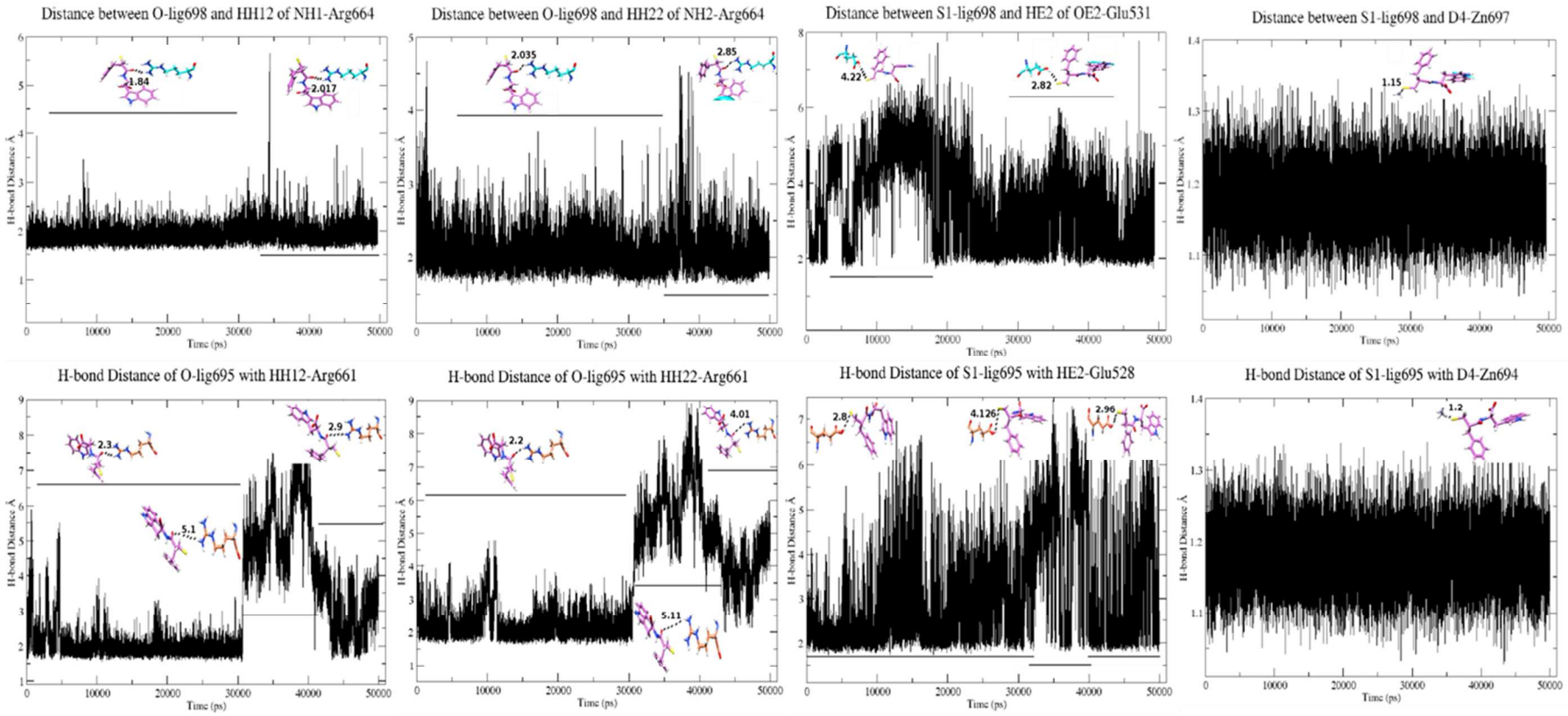

Figure-**7**: Upper and lower panels displayed the complexation of complound3 (pink) with NEP (cyan) and hNEP2 (orange), respectively. The lines over and under the graphs are the representatives of average pdbs generated for analysis of formation and deformation rates of important hydrogen bonds for interactions. Zn coordinated very effectively in both proteins; however, Arg664/661 mediated more potential hydrogen bonds towards NEP than hNEP2.

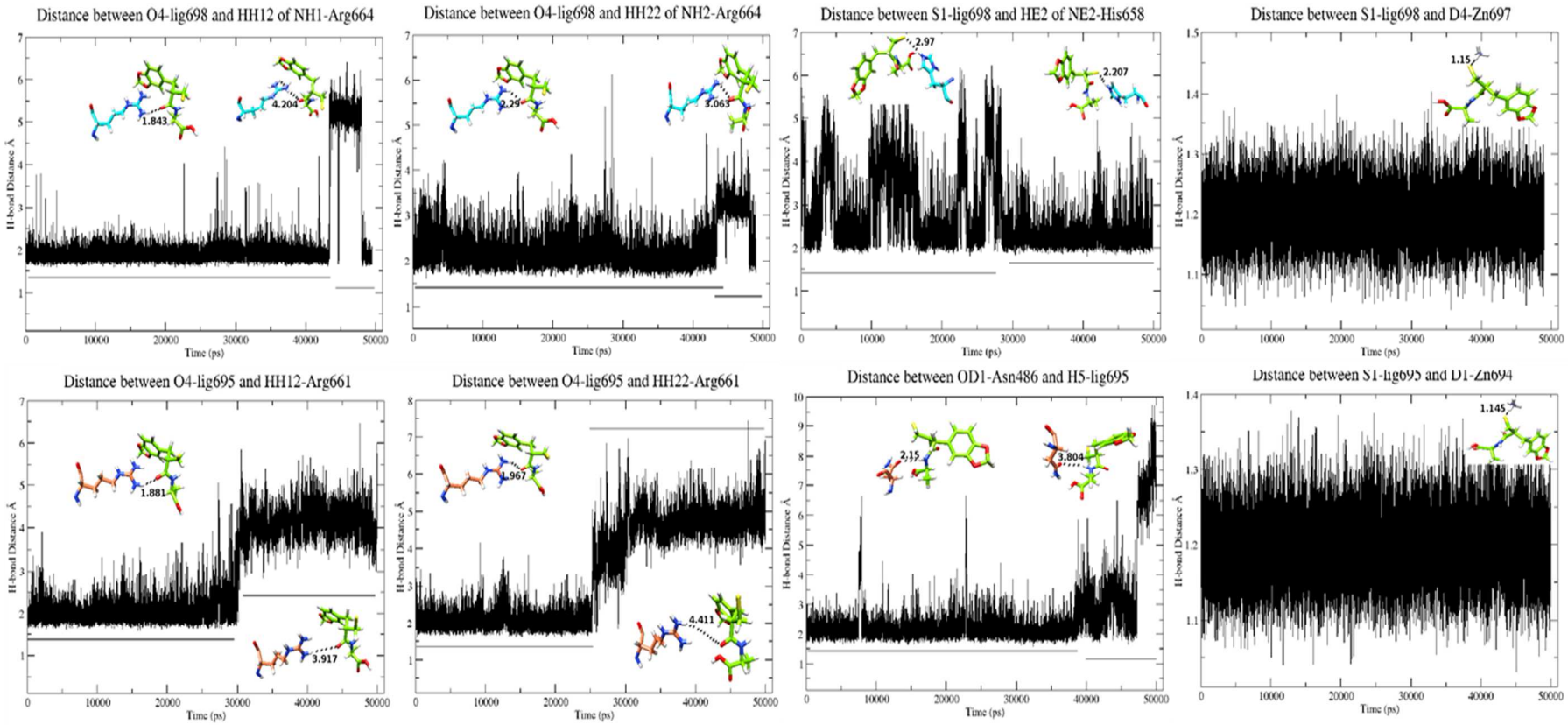

Figure-**8**: Fasidotrilat (parrot green) interacted with NEP (cyan) and hNEP2 (orange)through different degrees of interactions and occupancy of hydrogen bonds that are presented in upper (NEP) and lower (hNEP2) halves of figure. Average interaction diagrams of several ns were shown here by under and over lines, clearly demonstrate the change in bond over time.

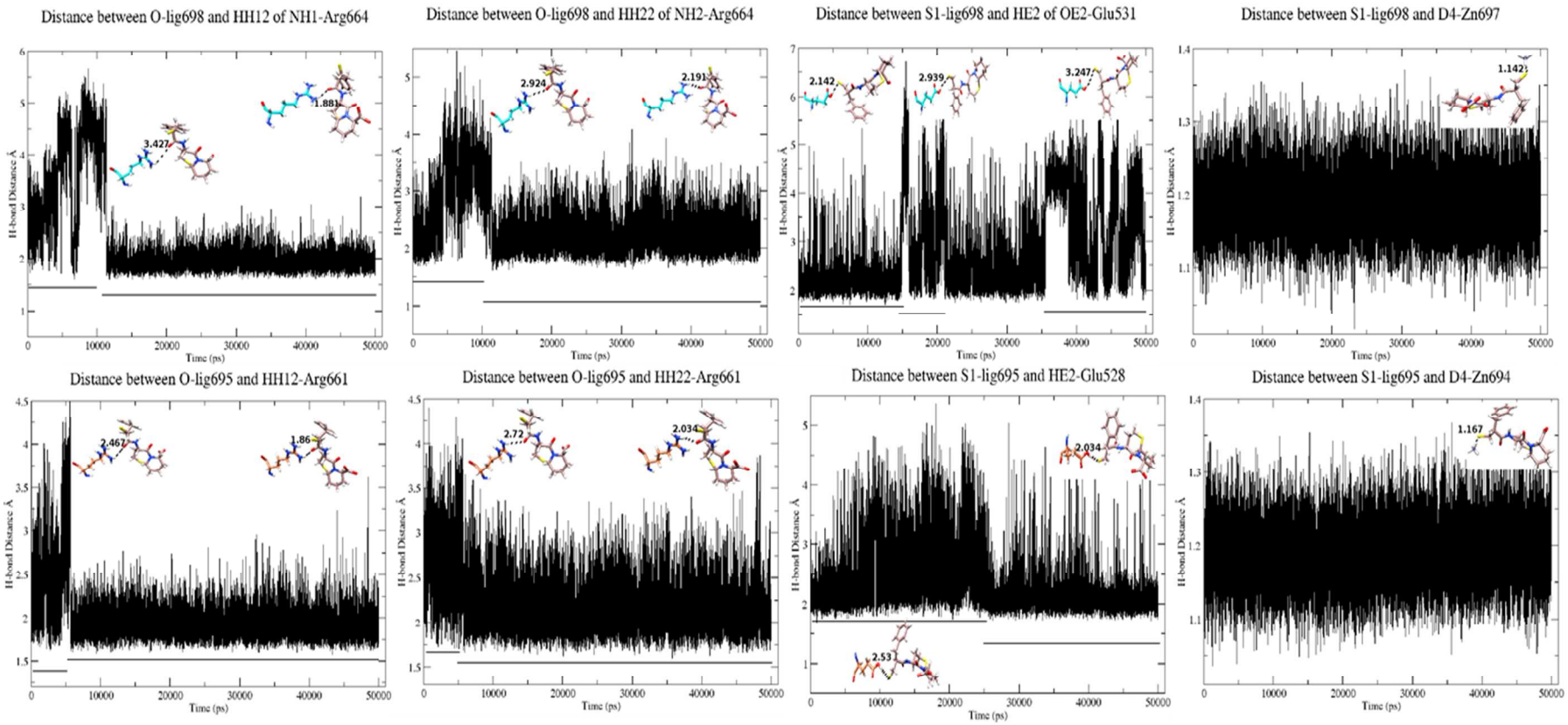

Figure-**9**: Interactions evaluation of omapatrilat (onion pink) through molecular dynamic simulation within NEP (cyan) and hNEP2 (orange) showed its quite equal potential activity against NEP and hNEP2. However, the rate of residual fluctuation was observed high in case of hNEP2 throughout the simulation.

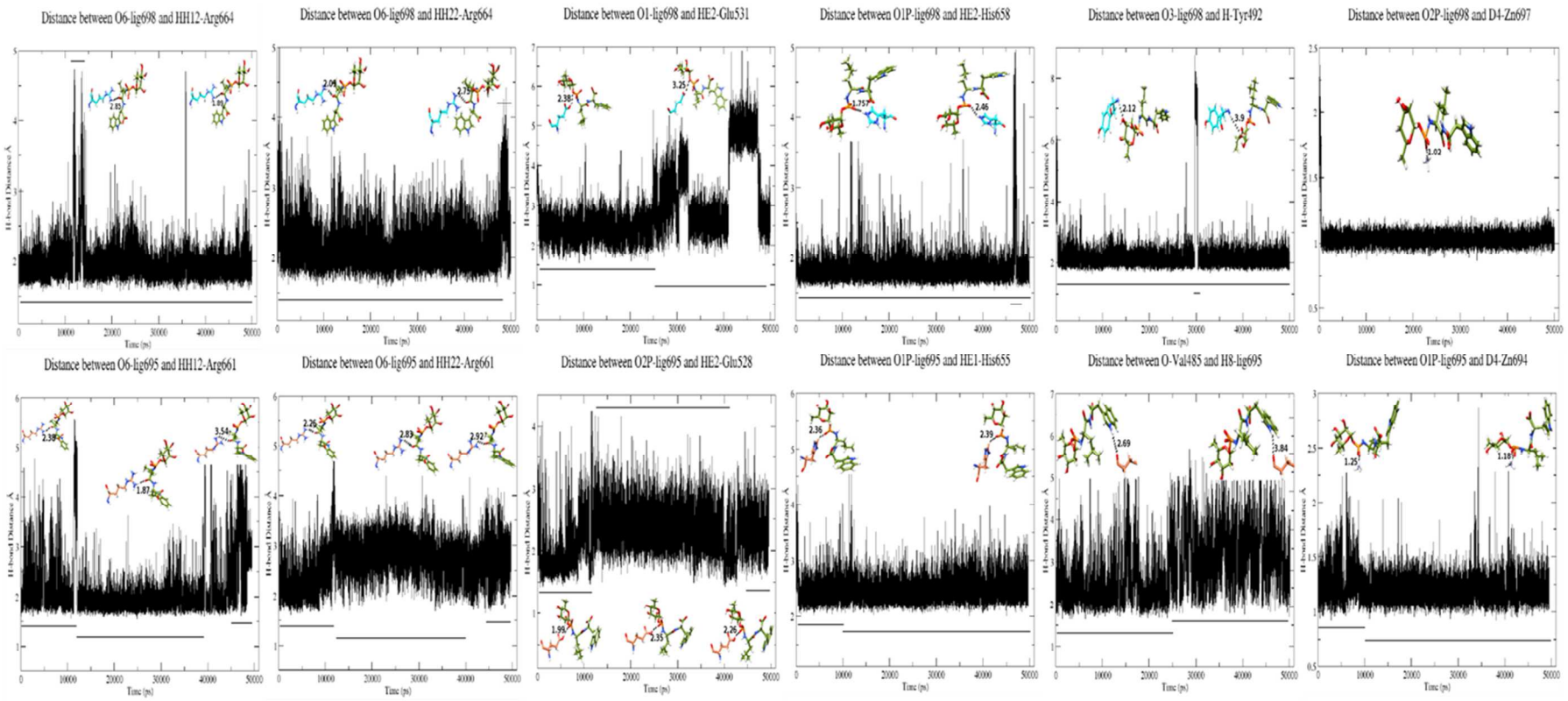

Figure-**10**: Olive green phosphoramidon in cyan NEP showed more persistent hydrogen bonds that were found to be same, we observed through its crystallographic structure. However, orange hNEP2 blocked less effectively by the same inhibitor with low degree occupancy of hydrogen bond with Val485 and fluctuating hydrogen bonds of Arg661 and Glu528 that than occurred with NEP protein.

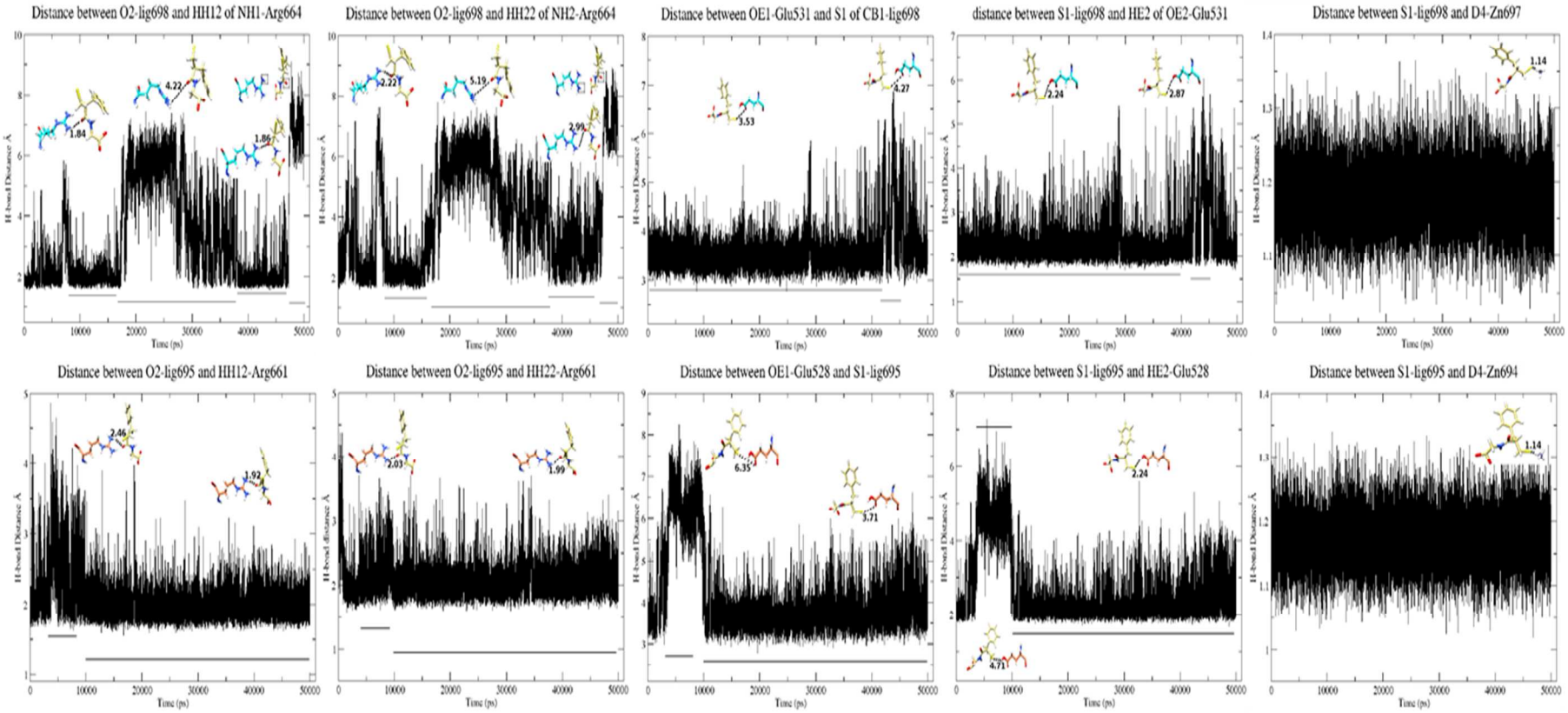

Figure-**11**: Computational interacting capability of thiorphan (yellow) was found to be in favor of hNEP2 (orange), however, experimental is in favor of NEP (cyan). These graphs of hydrogen bonds showed the same, having high occupancy rate of hydrogen bonds in hNEP2-thiorphan complex than in NEP-thiorphan coupled structure. This experimental to computational correlation was weak might be due to the physiological occurrence of blood brain barrier that hindered the extraction of near to real results.